Practical Papers, Articles and Application Notes

Flavio Canavero, Technical Editor

The content of this column is closely related to the main theme of the President's Message included in this issue, which discusses Electromagnetic Diversity as a paradigm for the future. The first paper below is entitled "Safety Evaluation of Walk-Through Metal Detectors" by D. Wu, R. Qiang, J. Chen, W. Kainz, and S. Seidman. I am indebted to Professor Robert Olsen, my predecessor, for having invited the authors and having conducted the review process of this contribution. This paper is related to the human safety assessment of magnetic devices of widespread use in locations accessed by the general public, such as airports or public buildings. In this case, a well-thought methodology helping to assess the devices against the exposure standards and to respond to possible public concerns is very important. In my opinion, this paper fulfils the scope of this column, since it provides an informative account of the methodologies of safety assessment to the EMC community at large, whose members - without being specialists of the field - will be curious I'm sure of having a better technical understanding of issues not always discussed with the proper rigor by the general press. Also, this paper provides an example of "compatibility" in a wider sense, that is, coexistence of systems of different natures (human and electronic).

The remaining two papers were originally presented the 2007 IEEE International Symposium on Electromagnetic Compatibility held last July in Hawaii. They are reprinted below with permission from the authors and the IEEE. They were presented in the Special Session on "Waveform Diversity" which was one of the distinctive new subjects of the Symposium. Waveform diversity is an emerging application that is becoming operational and refers to detection and/or identification of targets in interference and noise by means of a proper blend of various techniques based on spatial distribution of receivers and transmitters, different wave shapes, signal analysis in time and frequency domain, field polarization analysis, and other techniques. For example, if you are in a loud pub and want to listen to your conversation partner, you may start reading his/her lips, put your hand around your ear, move closer to your partner, etc. Waveform diversity exploits many sources and different techniques to gather the most information available from a target or a signal. (I realize that my example is rather mundane with respect to the abstract painting presented by our President, Andy Drozd, but this reflects the natural character difference between an engineer and an artist.)

The first paper on this topic, entitled "Waveform Diversity and Electromagnetic Compatibility," is by G. T. Capraro, I. Bradaric, and M. C. Wicks. It discusses the challenge that the integration of waveform diversity equipment for military and commercial applications brings to the EMC world. The second paper, entitled "Electromagnetic Diversity and EMI Implications for Multiple Co-sited Radars and Targeting Applications," is by Andrew L. Drozd, Irina Kasperovich, Ruixin Niu, Pramod K. Varshney and D. Weiner. It introduces the concept that orthogonality (in a broad sense, not only orthogonality of signals) must be preserved in the transmission schemes to assure the compatibility and coexistence of the diverse systems in a military or commercial scenario.

In conclusion, I encourage (as always) all readers to actively contribute to this column, either by submitting manuscripts they deem appropriate, or by nominating other authors having something exciting to share with the EMC community. I will follow all suggestions, and with the help of independent reviewers, I hope to provide a great variety of enjoyable and instructive papers. Please communicate with me, preferably by email at canavero@ieee.org.

Safety Evaluation of Walk-Through Metal Detectors

Dagang Wu, Rui Qiang, Ji Chen, Wolfgang Kainz, and Seth Seidman

Abstract—In this paper, we describe a procedure to evaluate the electrical current, induced by walk-through metal detectors electromagnetic emission, inside a human model for safety assessment. This procedure consists of the measurement of the magnetic field, the derivation of equivalent current source, and the calculation of induced current using the impedance method. This procedure is applied to determine, for a commercial walk-through metal detector, the induced currents within an anatomical human model.

Keywords—electromagnetic emission, induced current, equivalent current source

This work is partially supported by the National Science Foundation under grant number BES-0332957

I. Introduction

Walk-through metal detectors are an integral part of airport security surveillance systems and government buildings. Most of these metal detectors use the electromagnetic signal variations as a means to detect metal objects. A pair or pairs of transmitter/receivers are embedded in detector frames. If a metal object is presented inside the detector, a large electromagnetic signal variation is expected in the receiver. In principle, larger electromagnetic emission will lead to a higher sig-

nal to noise ratio, and consequently, more accurate results in metal detection.

While such electromagnetic emission can be used towards detecting metal objects, it also generates undesired electromagnetic energy depositions within human objects. To ensure public safety, exposure safety limits have been developed by the International Commission on Non-Ionizing Radiation Protection (ICNIRP) [1], IEEE C95.1 and IEEE C95.6. These guidelines define the maximum energy depositions within human subjects at different emission frequencies. Since the frequency of the electromagnetic emission for walk-through metal detectors are typically at low frequencies (i.e. below 10 kHz), the induced current strength should be used for emission safety assessment. However, for practical applications, it is impossible to directly measure the induced current strengths within human subjects; therefore, we use numerical methods to calculate the induced currents.

The purpose of this paper is to develop a procedure that can be used for accurate safety assessments for walk-through metal detector emissions. The procedure consists of three steps, first the measurement of the magnetic fields emitted by the walk-through metal detectors in absence of human subjects, second the development of an equivalent current source to represent the walk-through metal detectors emission, and third the calculation of the induced currents within a human model using the impedance method.

The following sections present these techniques and then perform the safety evaluation for a real world walk-through metal detector.

II. Methodology

We use the impedance method to calculate the induced current within human objects. In the impedance method, the external magnetic field is required. To obtain the external magnetic field, we first measure the magnetic field in the absence of the human subject. Based on the measured magnetic field distribution, we calculate an equivalent source to represent the original walk-through metal detector electromagnetic emission. Once the equivalent source is calculated, we can accurately evaluate the magnetic field distribution at any point within human subjects. Using the magnetic field generated by the equivalent source, we can calculate the induced currents within the human model using the impedance method. In the following, we describe the magnetic field measurement, the equivalent source development and the impedance method.

A. Measurement of Magnetic Field

Most walk-through metal detectors consist of two pylons as shown in Figure 1. To measure the magnetic field distribution within the walk-through metal detector pylons, an automatic three-axis measurement system was used. Details of the scanning system are outlined by J. Casamento in [2]. Typically, four planes of the magnetic field between the two pylons are measured for our applications. This system can simultaneously measure all three components of the magnetic field. The magnetic field is measured by two magnetic-field probes, a reference probe and measurement probe. A PC with custom made software controls the three motors to move the probe to any desired position. This system can measure the magnetic field in four channels; three channels are used to collect magnetic field strength in the *x*, *y*, and *z* directions, respectively. The fourth channel is used to determine the relative phase information for the *x*, *y*, and *z* channels. The fourth channel is referred to as the reference channel. Before a measurement begins, we put the reference probe on the position with a strong magnetic field to achieve the best phase measurement. Such a strong field typically resides at the center of one of the pylons on the outside of the walk through metal detector. This location avoids the possible collision between the moving probe and reference probe.

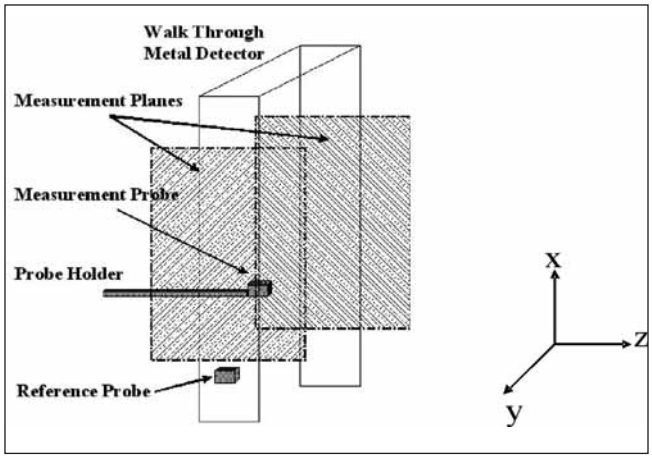

Figure 1. Illustration of magnetic field measurement.

Using this system, two sets of measurements are performed on two commercial walk-through metal detectors. For each of these detectors, the magnetic field distributions on four vertical planes, located at 5 cm, 10 cm, 15 cm and 20 cm parallel from the inside wall of one of the pylons, are measured. Each plane has a size of 120 cm in the horizontal direction and 180 cm in the vertical direction. The resolution of field measurement is 5 cm in all directions. Waveforms from each channel are recorded. The peak-to-peak signal strengths from the *x*, *y*, and *z* directions are first recorded. The relative phase information is then obtained by performing the correlation between the output waveform from the reference probe and the *x*, *y*, and *z* components from the measurement probe. Figure 2 shows the measured *y* directional magnetic field distribution at a plane that is 5 cm away from the pylon.

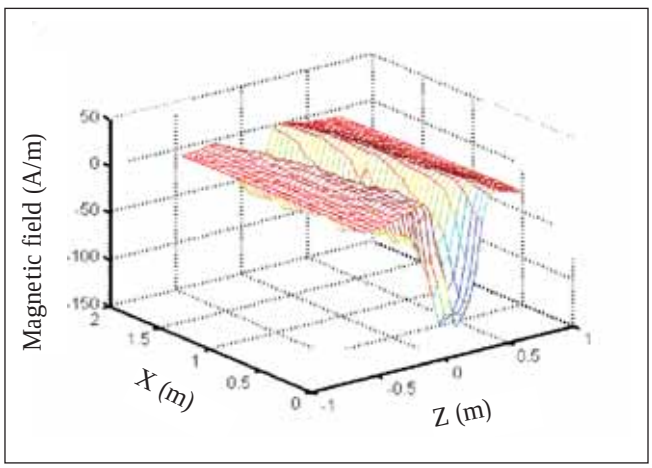

Figure 2. Measured y component of magnetic field distribution at a plane 5 cm away from one pylon.

B. Equivalent Source

Once the magnetic field distributions at four vertical planes are measured, we can derive an equivalent current source using the measured data. This equivalent source may not be the exact coil configurations by the manufacturer, but it can produce the same magnetic fields as that of the real coil configuration. Since the wavelength of the electromagnetic emission from the walk-through metal detectors is much larger than the size of the walk-through metal detectors, static approximation can be used. In particular, the Bio-Savart law is used to calculate the magnetic field generated by current sources.

To derive the equivalent current distribution on the pylons numerically, we first divide one side of the pylon into a two-dimensional grid. In each grid location, current in both vertical (x) and horizontal (z) directions are assumed, as shown in Figure 3. Denote $Jx = [J_x^1, J_x^2, \ldots, J_x^l]^T$ as the x directional currents, $Jy = [J_y^1, J_y^2 \ldots, J_y^m]^T$ as the y directional currents (are zero for our coordinate system as shown in Figure 3), and $Jz = [J_z^1, J_z^2, \ldots, J_z^n]^T$ as the z directional currents. The magnetic fields generated by such current segments are given by

$$\begin{bmatrix} H_x \\ H_y \\ H_z \end{bmatrix} = \begin{bmatrix} 0 & m_{xy} & m_{xz} \\ m_{yx} & 0 & m_{yz} \\ m_{zx} & m_{zy} & 0 \end{bmatrix} \begin{bmatrix} J_x \\ J_y \\ J_z \end{bmatrix} \tag{1}$$

where m_{xy} relates the x direction magnetic field generated by the y direction current following the Bio-Savart law. The dimension of the matrix depends on the number of observation points as well as the number of equivalent current points. The exact value of this term is determined from

$$\vec{\mathrm{H}} = \frac{1}{\mu}\vec{\mathrm{B}} = \nabla \times \vec{\mathrm{A}} = \int \frac{\mathrm{I}(\mathrm{r}')\vec{\mathrm{dl}}' \times \vec{\mathrm{R}}}{4\pi |\mathrm{R}|^3} \tag{2}$$

where the current strength $I(r')$ is assumed to be unitary, r and r' correspond to the observation and source point location and $\vec{R} = r - r'$ as shown in Figure 3. For our particular application, Equation (1) can also be written into $H = M \cdot J$, where the left side of the equation corresponds the measured magnetic fields. The right hand side term J is the unknown equivalent current distribution. Since the number of the measurement points may not be the exact number of the equivalent source points, the matrix itself is generally not a square matrix. To determine the equivalent current source which best matches the measured current distribution, we use the least square method to minimize the value of $|H - M \cdot J|$.

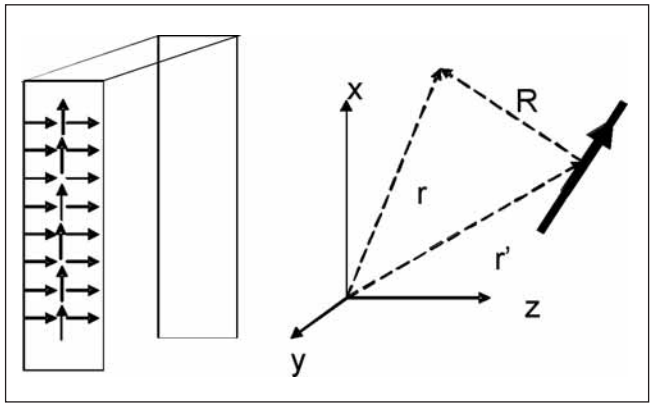

Figure 3. Illustration of the equivalent source discretization and the coordinate system.

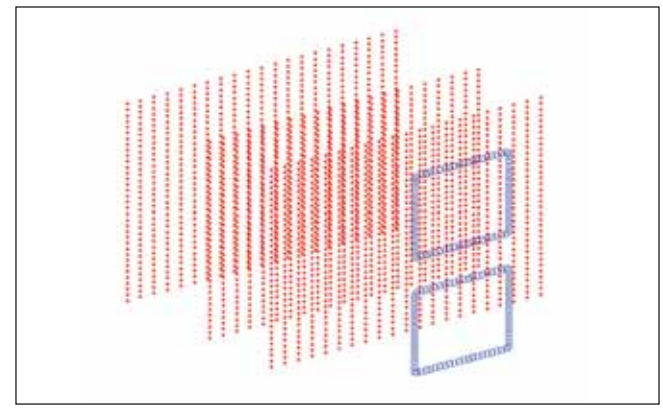

Figure 4. Geometry for a numerical experiment.

To verify the algorithm developed here, we first perform a numerical experiment. In this example, the magnetic fields generated by the two loop coils are calculated in three planes as shown in Figure 4. The method described above is used to calculate the equivalent source, which is confined in the same plane as the original source. In Figure 5, the equivalent current source in the plane of the original source is shown. For this ideal case, the algorithm can extract the original current distribution.

This algorithm is then used to extract the equivalent current source from the measured magnetic field generated by a walk-through metal detector. The extracted equivalent current distributions along three directions are shown in Figure 6. This current distribution may not be the exact representation of the original coil within the metal detector pylons. Nevertheless, it generates exactly the same magnetic fields as compared to the original measured magnetic field, as shown in Figure 7.

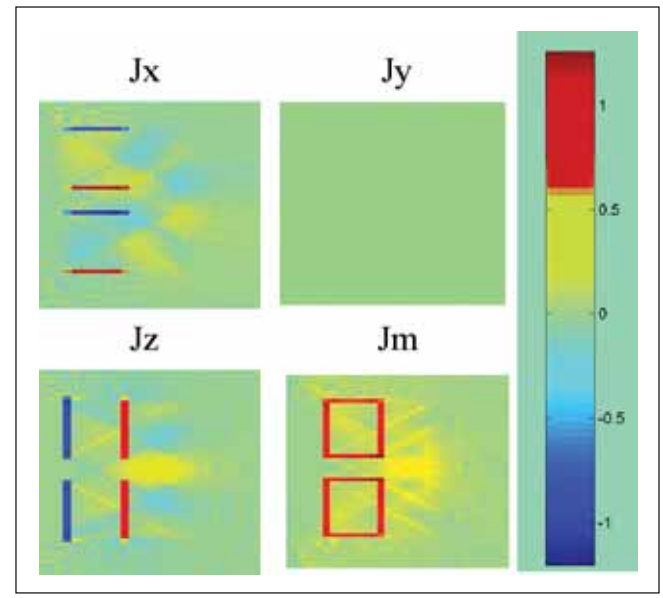

Figure 5. Equivalent current source generated by the algorithm shown as the three components (Jx, Jy, Jz) and the magnitude Jm.

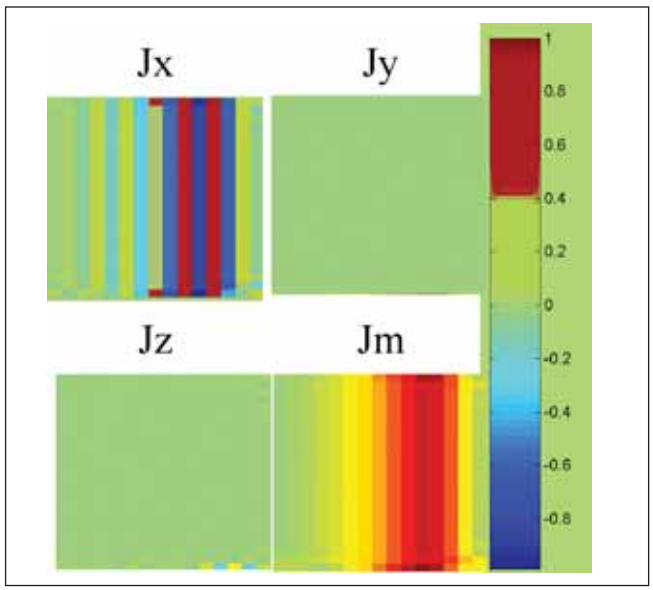

Figure 6. Equivalent source for one of the measured walk-through metal detectors shown as the three components (Jx, Jy, Jz) and the magnitude Jm.

C. Impedance Method

After the equivalent current source is obtained for the measured magnetic field, we can perform the safety assessments for various walk-through metal detectors using numerical techniques. Among the methods proposed for bio-electromagnetic problems, the time-domain finite difference and the impedance method have been proven to be effective for complicated 3-D bodies. At the frequency of our interests, the problem is quasi-static and the impedance method [3]–[5] is especially attractive for our application.

Based on the impedance method, at an extremely low frequency, the anatomical model is represented by a 3-D network of impedances. In this model, which is constructed using a 3-D Cartesian grid as shown in Figure 8, each cell has a shape of a parallelepiped and with impedance in the x direction is given by:

$$Z_x = \frac{\Delta x}{\Delta y \Delta z(\sigma + j\omega\varepsilon)} \tag{3}$$

where σ and ε are the conductivity and permittivity of the cell and Δx, Δy, Δz are the size of the voxels in the x, y, z directions. Similar expressions can be derived for the y and z direction impedances.

For each loop, Kirchhoff's voltage equation is used with an electromotive force generated by magnetic fields ($\overline{B}$):

$$emf = -\frac{\partial}{\partial t}\iint \vec{B}.d\vec{s} \tag{4}$$

Applying Kirchhoff's voltage equations to each loop, we derive the following system of equations:

$$\sum_{n=1}^{3} a_{mn}^{i,j,k} x_n(i, j, k) = emf_m; \quad 1 \le m \le 3 \tag{5}$$

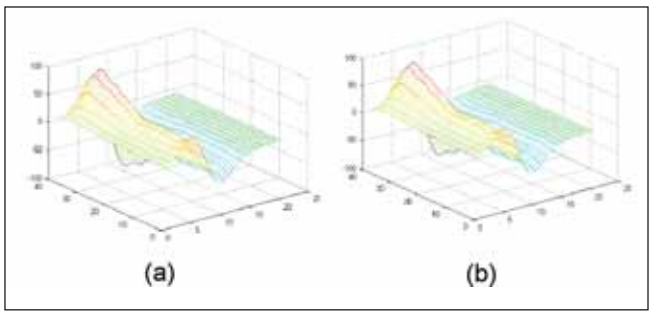

Figure 7. Comparison between (a) measured magnetic field (A/m) and (b) equivalent current source generated magnetic field. (A/m)

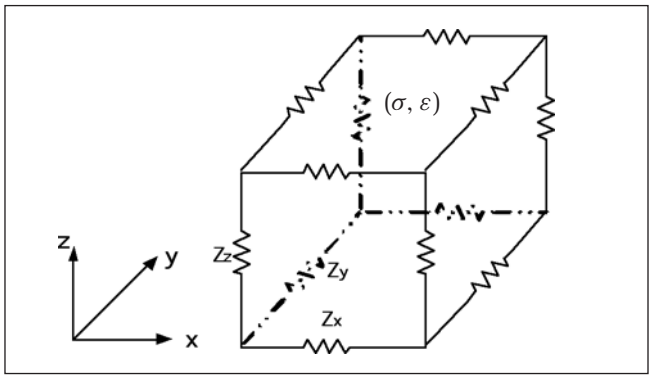

Figure 8. Equivalent circuit network for impedance method.

where $x_{1,2,3}$ stands for the loop current along the x, y, z direction and $a_{mn}^{i,j,k}$ are the coefficients from Kirchhoff's voltage equations. This system of equations can be solved using the successive over-relaxation method. Consequently, the line currents can be obtained from the known loop currents. The current density and the induced electric field can then be calculated from the line currents.

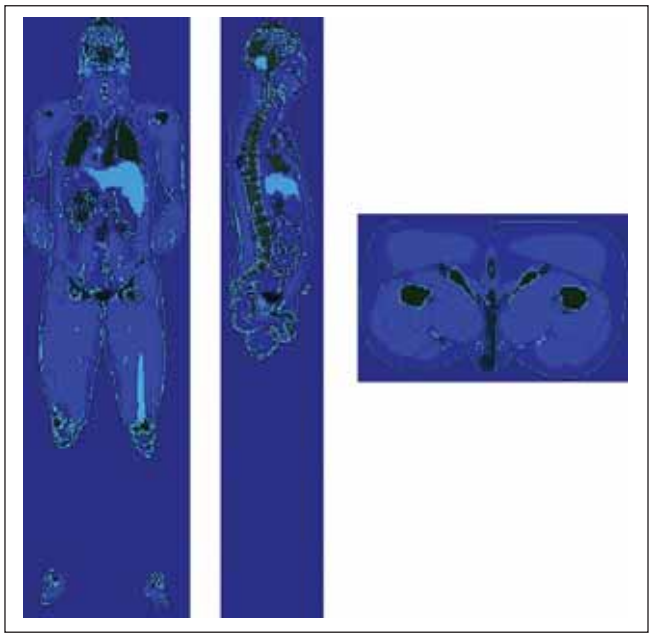

Figure 9. Three slides of the human model used in this study.

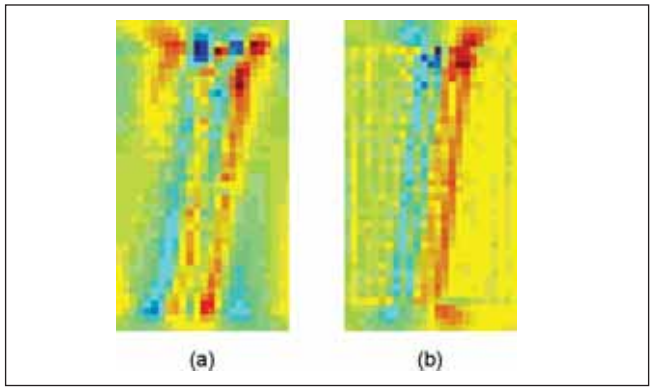

Figure 10. Equivalent current sources on one of the pylon (a) x direction current (b) z direction current.

III. Calculation of Induced Current Within a Human Anatomical Model

With the methods described above, we now calculate the induced current density within a human subject model. The human model used in this study is obtained from Brooks Air Force Laboratory. This model has a resolution of 3 mm in all directions. It consists of over 40 different tissues. Three slides through the center of the anatomical models are shown in Figure 9. The electrical properties of the human body are modeled in terms of multiple Cole-Cole dispersion models [6]–[7]. In this model, the tissue response is modeled by the relaxation theory. The complex permittivity of the biological tissue is described as:

$$\varepsilon_r^*(\omega) = \varepsilon_\infty + \sum_{n=1}^{4} \frac{\Delta\varepsilon_n}{1 + [j(\omega/2\pi)\tau_n]^{\alpha_n}} + \frac{\sigma}{j\omega\varepsilon_0} \qquad (6)$$

where ε_∞ is the permittivity in the high frequency limit, σ is the static ionic conductivity, τ_n the relaxation time in the dispersion region n, and $\Delta\varepsilon_n$ the drop in permittivity. The values of these parameters are available in [6].

To perform the induced current density calculation, first the magnetic fields in four vertical planes between two pylons are measured. Based on the measured magnitude field distribution, we calculate the equivalent current source that can generate the exact same magnetic field distribution. For this particular walk-through metal detector, only one pylon emits electromagnetic signals, and therefore, the equivalent current is evaluated only for one pylon. Also, since the values for the *y* direction current is much smaller than those for the *x* and *z* directions, only *x* and *z* equivalent currents are used. The equivalent currents in the *x* and *z* directions are shown in Figure 10.

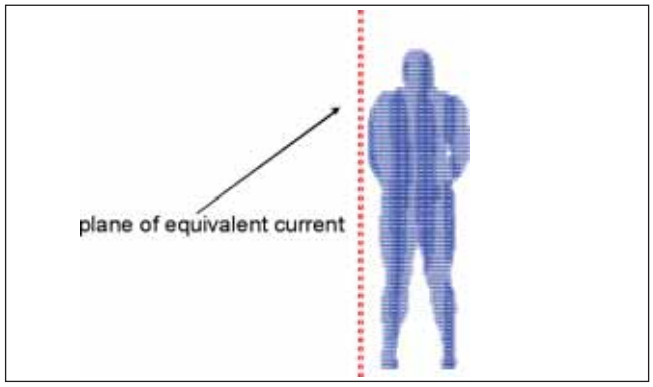

Figure 11. Plane of equivalent current source and its relative position of the human model.

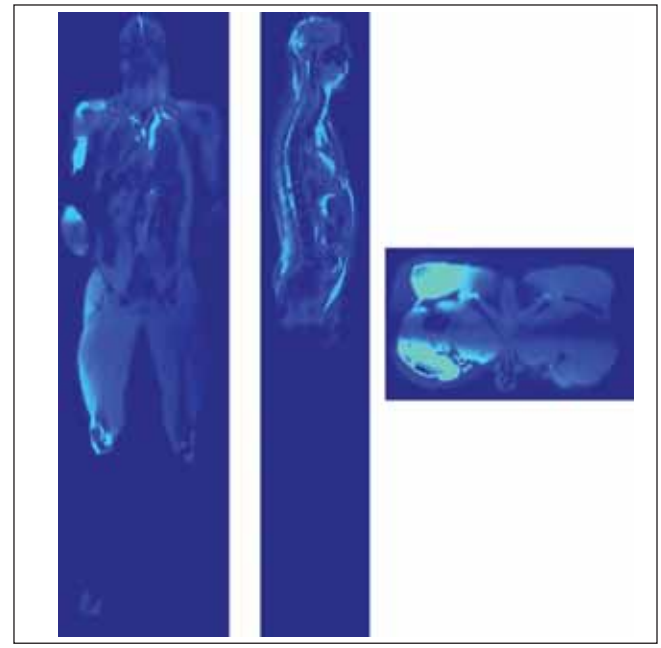

Figure 12. Induced current in three center planes.

With the obtained equivalent source, we calculate the induced current density using the impedance method. For this particular simulation, the spacing between the human model and the plane of equivalent current source is chosen 3 cm as shown in Figure 11. We assume that the electromagnetic emission frequency is at 60 Hz. In the impedance simulation, a total number of 3500 iterations is required to reach a relative error of less than 5×10^{-5}. On a regular PC, this takes about 12 hours of simulation time and around 1.2 GB of computer memory. From the simulation, we found that the maximum induced current density is at 3.5×10^{-4} A/m^2.

The induced currents in the three center planes are shown in Figure 12. As we expected, the stronger induced currents are observed at the left side of the human model.

IV. Conclusions

We developed a novel method to evaluate the exposure situation of humans in walk-through metal detectors. The developed method could also be used for other walk through security systems. The equivalent source model is able to exactly reproduce the magnetic field distributions and to calculate the exposure situation for different anatomical models exposed to different walk through metal detectors. It is the first time that a method was developed which is able to exactly calculate the induced current density based on measurements of real walk trough metal detectors. The deployment of more security systems using stronger magnetic fields makes it necessary to evaluate the exposure situation of people of different ages and sizes in a most efficient and accurate way. We will use the developed method to evaluate the exposure situations of children, pregnant women and adults in different commercially used walk through metal detectors and other walk through security systems.

Disclaimer

The opinions and conclusions stated in this paper are those of the authors and do not represent the official position of the Department of Health and Human Services.

References

[1] International Commission on Non-Ionizing Radiation Protection (ICNIRP) 1998a Guidelines for limiting exposure to time-varying electric, magnetic, and electromagnetic fields (up to 300 GHz) Health Phys. 74 494–522m 1998.

[2] J. Casamento, "Characterizing electromagnetic fields of common electronic article surveillance systems," *Compliance Eng.*, vol. 16, pp. 42–52, Sept. 1999.

[3] O.P. Gandhi, J.F. DeFord, and H. Kanai, "Impedance method for calculation of power deposition patterns in magnetically induced hyperthermia," *IEEE Trans. Biomed. Eng.*, vol. BME-31, pp. 644–651, 1984.

[4] N. Orcutt and O.P. Gandhi, "A 3-D impedance method to calculate power deposition in biological bodies subject to time varying magnetic fields," *IEEE Trans. Biomed. Eng.*, vol. 35, pp. 577–583, Aug. 1988.

[5] O.P. Ghandhi, "Some numerical methods for dosimetry: Extremely low frequencies to microwave frequencies," *Radio Sci.*, vol. 30, no. 1, pp. 161–177, 1995.

[6] S. Gabriel, R.W. Lau, and C. Gabriel, "The dielectric properties of biological tissues: III. Parametric models for the frequency spectrum of tissues," *Phys. Med. Biol.*, vol. 41, pp. 2271–2293, 1996.

[7] K.S. Cole and R.H. Cole, "Dispersion and absorption in dielectrics: alternating current characteristics," *J. Chem. Phys.*, vol. 9, p. 341, 1941.

Dagang Wu, Rui Qiang, and Ji Chen
Department of Electrical & Computer Engineering
University of Houston
Houston, TX, 77204 USA
Dagang.Wu (Rui.Qiang, Ji.Chen)@mail.uh.edu

Wolfgang Kainz and Seth Seidman
U.S. Food and Drug Administration (FDA)
Center for Devices and Radiological Health, FDA
10903 New Hampshire Avenue, WO62-1131
Silver Spring, MD 20993-0002
Wolfgang.Kainz (Seth.Seidman)@fda.hhs.gov

Biographies

Dagang Wu (S'99) was born in Nanjing, China, on November 10, 1978. He received the B.S. and M.S. degrees in electrical engineering from Southeast University, Nanjing, China, in 1999 and 2002, respectively. Since September 2002, he has been a Research Assistant in the Department of Electrical and Computer Engineering at the University of Houston, Texas. His current research interests include computational electromagnetics, bio-electromagnetics and numerical LWD/MWD modeling.

Rui Qiang (S'2003) received the B.S. and M.S. degrees in 1999 and 2002, respectively, from the Department of Radio Engineering, Southeast University, Nanjing, China. He is currently working toward a Ph.D. degree in the Department of Electrical and Computer Engineering at the University of Houston, Texas. His current research interests include FDTD methods, nanoscale frequency selective surface (FSS) modeling and DNG medium modeling.

Ji Chen received the Bachelor's degree from Huazhong University of Science and Technology, Wuhan, Hubei, China, in 1989, the Master's degree from McMaster University, Hamilton, ON, Canada, in 1994, and the Ph.D. degree from the University of Illinois at Urbana-Champaign in 1998, all in electrical engineering. He is currently an Assistant Professor with the Department of Electrical and Computer Engineering at the University of Houston, Texas. Prior to joining the University of Houston, from 1998 to 2001, he was a Staff Engineer with Motorola Personal Communication Research Laboratories, Chicago, Illinois. Dr. Chen is the recipient of the 2000 Motorola Engineering Award.

Wolfgang Kainz received the M.S. and Ph.D. degrees in Electrical Engineering from the Vienna University of Technology. After working for the Austrian Research Center Seibersdorf (ARCS) on electromagnetic compatibility of electronic implants and exposure setups for bio-experiments, he joined The Foundation for Research on Information Technologies in Society – IT'IS (Zurich, Switzerland) as Associate Director. He managed IT'IS together with Professor Niels Kuster (IT'IS Director and Founder) and worked on the development of in-vivo and in-vitro exposure setups for bio-experiments. In 2002, he moved to the USA where he is currently working for the U.S. Food and Drug Administration in the Center for Devices and Radiological Health. He is Chairman of the IEEE Standards Coordination Committee 34, Sub-Committee 2, which develops compliance techniques for wireless devices. His research interest is focused on safety and effectiveness of medical devices and safety in electromagnetic fields. This includes 1) computational electrodynamics (FDTD and FEM simulations) for safety and effectiveness evaluations, 2) MRI - Magnetic Resonance Imaging safety, 3) performance and safety of wireless technology used in medical devices, 4) electromagnetic compatibility of medical devices, especially electronic implants, and 5) dosimetric exposure assessments.

Seth J. Seidman received the B.S. degree in electrical engineering from the University of Maryland, College Park, Maryland. After graduation, he joined the U.S. Food and Drug Administration in the Center for Devices and Radiological Health to conduct research concerning medical device safety. His current research involves electromagnetic compatibility (EMC) between medical devices and current wireless technologies such as Bluetooth and 802.11. The primary goal of this research is to identify serious incompatibilities and dangers of allowing such technologies around hospitals and patients with medical devices. He has also performed EMC research for walk-through and hand-held metal detectors and their interactions with medical devices.